BIOCHEMISTRY
including biophysical chemistry & molecular biology

Article

pubs.acs.org/biochemistry

Active Site Substitution A82W Improves the Regioselectivity of Steroid Hydroxylation by Cytochrome P450 BM3 Mutants As Rationalized by Spin Relaxation Nuclear Magnetic Resonance Studies

V. Rea,[†] A. J. Kolkman,[‡] E. Vottero,[†] E. J. Stronks,[‡] K. A. M. Ampt,[‡] M. Honing,[§] N. P. E. Vermeulen,[†] S. S. Wijmenga,[‡] and J. N. M. Commandeur*[,†]

[†]LACDR/Division of Molecular Toxicology, Department of Pharmacochemistry, VU University Amsterdam, De Boelelaan 1083, 1081 HV Amsterdam, The Netherlands

[‡]Institute for Molecules and Materials, Department of Biophysical Chemistry, Radboud University Nijmegen, Heyendaalseweg 135, 6525 AJ Nijmegen, The Netherlands

[§]MSD, Merck Research Laboratories, Medicinal Chemistry Oss, Molenstraat 110, 5342 CC Oss, The Netherlands

Supporting Information

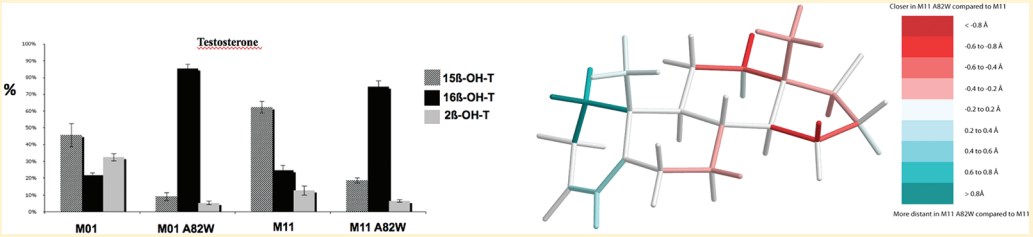

ABSTRACT: Cytochrome P450 BM3 from *Bacillus megaterium* is a monooxygenase with great potential for biotechnological applications. In this paper, we present engineered drug-metabolizing P450 BM3 mutants as a novel tool for regioselective hydroxylation of steroids at position 16β. In particular, we show that by replacing alanine at position 82 with a tryptophan in P450 BM3 mutants M01 and M11, the selectivity toward 16β-hydroxylation for both testosterone and norethisterone was strongly increased. The A82W mutation led to a $\leq$42-fold increase in V_{max} for 16β-hydroxylation of these steroids. Moreover, this mutation improves the coupling efficiency of the enzyme, which might be explained by a more efficient exclusion of water from the active site. The substrate affinity for testosterone increased at least 9-fold in M11 with tryptophan at position 82. A change in the orientation of testosterone in the M11 A82W mutant as compared to the orientation in M11 was observed by T_1 paramagnetic relaxation nuclear magnetic resonance. Testosterone is oriented in M11 with both the A- and D-ring protons closest to the heme iron. Substituting alanine at position 82 with tryptophan results in increased A-ring proton−iron distances, consistent with the relative decrease in the level of A-ring hydroxylation at position 2β.

Cytochrome P450s (CYPs) constitute a large superfamily of monooxygenases that are involved in the oxidation and reduction of a wide variety of primary and secondary metabolites and in the biotransformation of xenobiotics.[1] Because of their broad substrate range and catalytic diversity, there is an increasing interest to use P450 enzymes in biotechnology.[2−4] Among others, their application in the production of pharmaceuticals and the optimization of lead compounds by P450 enzymes has been explored recently.[5] An important class of compounds for which P450s play an important role in biosynthesis and catabolism consists of steroids, which have a wide range of therapeutic activities, including anti-inflammatory, immunosuppressive, progestational, diuretic, anabolic, and contraceptive activities.[6] Both chemical and biological approaches are used for the production of steroids. Chemical synthesis of steroids requires highly complicated, multistep schemes that are expensive and time-consuming. Many microorganisms that are able to hydroxylate steroids at specific positions have been identified. Therefore, microbial biosynthesis can be an efficient alternative for large-scale synthesis of steroid drugs.[6] Very often, an early step in these biotransformations is a regio- and stereospecific hydroxylation of a steroid core by microbial P450s. However, microbial hydroxylation of steroids is often hampered by the formation of byproduct because of nonspecific and secondary metabolism.

Another approach is to clone a genetically engineered steroid hydroxylating P450 into a suitable expression system that is devoid of secondary steroid catabolism. Several mammalian P450s are known to regioselectively hydroxylate steroids.[7] However, because of their low stability and catalytic activity, they are not very suitable as biocatalysts for steroid hydroxylations.[8,9] Genetically engineered bacterial P450s are

Received: September 14, 2011
Revised: December 23, 2011
Published: December 28, 2011

often much more stable and exhibit higher catalytic activities, which make them more promising candidates for biocatalysis.[10] Of the bacterial P450s, cytochrome P450 BM3 (P450 BM3 or CYP102A1) from *Bacillus megaterium* is considered as one of the most promising monooxygenases for biotechnological applications because it is the most active P450 so far identified.[8] Wild-type P450 BM3 catalyzes the hydroxylation of long-chain fatty acids at subterminal positions (ω-1 to ω-3). By site-directed and random mutagenesis, the substrate specificity of P450 BM3 has been expanded to include alkanes, indoles, short- and medium-chain fatty acids, polycyclic aromatic hydrocarbons, and drugs.[4,11,12] In recent years, several mutants of P450 BM3 has been shown to catalyze the hydroxylation of steroids. A triple mutant of P450 BM3 (R47L/F87V/L188Q) and several mutants obtained by random mutagenesis were found to hydroxylate testosterone, norethisterone, nandrolone, progesterone, and androstendione.[13−15] However, the regioselectivity of steroid hydroxylation by most P450 BM3 mutants was still poor, resulting in multiple mono- and dihydroxy metabolites. Testosterone hydroxylation by P450 BM3 mutants has been shown to occur at positions 2β, 15β, and 16β,[23,25] and recently, other mutants that are highly selective for 2β- and 15β-hydroxylation were obtained.[23]

Previously, it was shown that increasing the size of the active site residue at position 82 in wild-type P450 BM3, by mutations A82F and A82W, strongly improves binding of fatty acids and indoles, resulting in substantially increased catalytic efficiency and binding affinity.[16] However, no significant change in regioselectivity in metabolism was observed. The aim of this study was to investigate whether the introduction of the A82W mutation into P450 BM3 mutants M01 and M11 affects the activity and/or regioselectivity of steroid hydroxylation. Two steroid substrates, testosterone and norethisterone, were selected because they have been shown to be metabolized to three and two monohydroxy metabolites, respectively, by M01 and M11.[15,17]

The orientation of a substrate in the active site of P450 enzymes can be determined by T_1 paramagnetic relaxation nuclear magnetic resonance (NMR).[18] T_1 paramagnetic relaxation experiments have been used previously to determine proton−heme iron distances in P450 enzymes,[19−21] which give information about the orientation(s) and mobility of ligands in the active site of P450 enzymes. For P450 BM3, these experiments have been used to determine the substrate orientation of the highly flexible substrates lauric acid and 12-bromolauric acid.[19,22,23] Steroid compounds might be more informative compounds for determining the substrate orientation because they are large compounds with a dense network of protons; hence, many protons can be used to determine the proton−heme iron distances. Because they are rigid structures, the obtained distances give more information about the binding and mobility in the active site, rather than the conformational flexibility of the steroid. No T_1 paramagnetic relaxation NMR experiments have been used to study the binding of steroids to P450 BM3s. The only T_1 paramagnetic relaxation NMR study addressing the binding orientation of steroids in P450s involved binding of testosterone to a genetically engineered mutant of CYP2D6 (F438I), which had acquired the ability to catalyze testosterone hydroxylation.[24] In this study, Smith et al. determined the distances from several protons of testosterone to the heme iron of the CYP2D6 mutant, including protons H2β, H15β, and H16β. Recently, we and others have demonstrated that BM3 mutants catalyze testosterone hydroxylation only at these three positions but with different regioselectivities.[15,23,25] In the study presented here, T_1 paramagnetic relaxation NMR studies were performed to investigate whether the change in the regioselectivity of testosterone hydroxylation that is observed in the A82W mutants can be explained by different binding orientations of testosterone.

MATERIALS AND METHODS

Chemicals. D-Glucose 6-phosphate dipotassium salt hydrate (100% pure), glucose-6-phosphate dehydrogenase, dimethyl sulfoxide-d_6 (100% pure, 99.9 atom % D), carbon monoxide (>99% pure), and sodium dithionite (>86% pure) were purchased from Sigma-Aldrich (Schnelldorf, Germany). All other chemicals were of analytical grade and obtained from standard suppliers.

Site-Directed Mutagenesis. The A82W mutation was introduced by site-directed mutagenesis in two templates, M11 (R47L, E64G, F81I, F87V, E143G, L188Q, E267V, and G415S) and M01 (R47L, F87V, L188Q, and E267V).[10] The mutation was introduced into the pBS-p450 BM3 mutant using the QuikChange XL site-directed mutagenesis kit (Stratagene). The sequence of the forward primer for the mutation in M11 was 5′-GT.CAA.GCG.CTT.AAA.TTT.GTT.CGC.GA-T.ATT.***TGG***.GGA.GAC.GGG-3′, with the altered residue shown in bold italics. The reverse primer for this positions was 5′-CCC.GTC.TCC.***CCA***.AAT.ATC.GCG.AAC.AAA.TT-T.AAG.CGC.TTG.AC-3′. The sequences of the primers for the mutation in M01 were as follows: forward primer, 5′-GT.CAA.GCG.CTT.AAA.TTT.GTT.CGC.GAT.TTT.***TGG***.G-GA.GAC.GGG-3′; reverse primer, 5′-CCC.GTC.TCC.***CCA***.AAA.ATC.GCG.AAC.AAA.TT-T.AAG.CGC.TTG.AC-3′. The PCR product was digested with EcoRI and BamHI restriction enzymes and cloned into a pET28a+ vector, which encodes an N-terminal His tag to allow facile purification. The desired mutations were confirmed by DNA sequencing of the heme domain (Baseclear, Leiden, The Netherlands).

Expression, Isolation, and Purification of P450 BM3 Mutants. Expression of the CYP102A1 mutants was performed by transforming competent *Escherichia coli* BL21 cells with the corresponding pET28+ vectors, as described previously.[25] Proteins were purified using Ni-NTA agarose,[25] after which P450 concentrations were determined according to methods described by Omura and Sato.[26] The purity of the enzymes was checked by sodium dodecyl sulfate−polyacrylamide gel electrophoresis on a 12% gel with Coomassie staining.

Determination of the Kinetic Parameters of the Biotransformation of Testosterone and Norethisterone by P450 BM3 Mutants. Testosterone and norethisterone incubations were performed in 100 mM potassium phosphate buffer (pH 7.4), with 200 nM purified P450 BM3 mutants.[10] The final volume of the incubation was 200 μL, with a substrate concentration of 200 μM. The reactions were initiated by addition of an NADPH regenerating system (final concentrations of 0.2 mM NADPH, 0.3 mM glucose 6-phosphate, and 0.4 unit/mL glucose-6-phosphate dehydrogenase). The reaction was allowed to proceed for 60 min at 25 °C and terminated by the addition of 200 μL of cold methanol. Precipitated protein was removed by centrifugation (15 min at 14000*g*), and the supernatant was analyzed by UPLC. Metabolites were separated using a C18 column (Zorbax Eclipse XDB-C18, 4.6 mm × 50 mm, 1.8 μm, Agilent

Technologies) with a flow rate of 1 mL/min, isocratic 60% B (99% MeOH, 0.8% H_2O, and 0.2% formic acid), 40% A (99% H_2O, 0.8% MeOH, and 0.2% formic acid), and UV detection at 254 nm.

To determine the kinetic parameters, the ranges where the enzyme activity is linear with enzyme concentration and incubation time were first determined. On the basis of these experiments (data not shown), the most suitable conditions were chosen for the determination of the kinetic parameters. The enzyme concentration was 300 nM, and the incubation time was 10 min; 10 substrate concentrations were used in the ranges of 20−200 μM for testosterone and 10−250 μM for norethisterone. Specific activities were calculated and plotted versus substrate concentration. The data were fitted with the Michaelis−Menten equation, using OriginPro8.

Determination of Coupling Efficiency. To measure the NADPH consumption rate, the P450 BM3 mutant (final concentration of 200 nM) was mixed with 870 μL of 100 mM potassium phosphate buffer (pH 7.4) containing 200 μM testosterone or norethisterone in DMSO (final concentration of 2%). The reaction was started by adding 200 μM NADPH. NADPH consumption was monitored at 340 nm with a Libra S12 Biochrom spectrophotometer at 25 °C for 10 min. The NADPH concentration was calculated using an ε of 6200 M^{-1} cm^{-1}.[27]

To measure the coupling efficiency, product formation and substrate consumption were quantified by high-performance liquid chromatography. The percentage of coupling was determined by the ratio of the amount of product formed and the amount of NADPH consumed.

Preparative-Scale Biotransformation and Isolation of Testosterone Metabolites. The testosterone metabolites were produced on a preparative scale by large-scale incubation with M11 as a biocatalyst. A 50 mL reaction volume containing 250 nM M11 mutant, 500 μM testosterone, and NADPH regenerating system was prepared in 100 mM potassium phosphate buffer (pH 7.4). The reaction was allowed to continue for 3 h at 25 °C. The reaction products were extracted by using 3 × 100 mL of dichloromethane. The organic layers were combined and evaporated using a rotary evaporator. The dried product was redissolved in 0.5 mL of DMSO and injected into a Waters preparative LC system, equipped with an HP liquid handler for injection and fractionation, a Waters Xbridge Prep C18-MS (10 mm × 55 mm, 5 μm particles) column, and a Waters photodiode array detector. At a flow rate of 5 mL/min, the following gradient was used: from 0 to 1 min, 100% A (99.95% H_2O and 0.05% TFA); from 1 to 15 min, linear increase to 60% B (30% MeOH, 60% acetonitrile, 10% H_2O, and 0.05% TFA); from 15 to 15.5 min, linear increase to 100% B; constant for 2 min; and finally a column equilibration time of 2 min with 100% A. Fractions were collected, triggered by UV absorbance at 210 nm. All fractions were evaporated to dryness and redissolved in 550 μL of DMSO-d_6 with tetramethylsilane for internal referencing in the subsequent NMR analysis.

Structural Characterization of Testosterone Metabolites by NMR. The chemical structures of the testosterone metabolites formed by M11 were determined by a combination of one-dimensional (1D) ^{1}H, ^{1}H−^{1}H DQF-COSY, ^{1}H−^{13}C HSQC, ^{1}H−^{13}C HMQC, ^{1}H−^{13}C HMBC, and ^{1}H−^{1}H NOESY NMR experiments. The experiments were conducted on a Varian INOVA 500 MHz spectrometer operating at a ^{1}H frequency of 499.85 MHz and a Varian INOVA 600 MHz spectrometer operating at a ^{1}H frequency of 599.76 MHz, both equipped with a 5 mm probe and operating at 298 K. The proton and carbon chemical shifts were referenced to the internal reference TMS (proton, δ 0.00; carbon, δ 0.00). Data were processed using ACDLabs/SpecManager, version 12.01.

UV−Vis Spectroscopy. UV−visible spectra were recorded using a Varian Cary 300 UV−visible spectrophotometer with a temperature controller. All spectra were recorded at 25 °C in quartz cuvettes (10 mm path length) for samples containing 100 mM phosphate buffer (pH 7.4). UV−vis spectroscopy was used to determine the concentration of enzyme, by measuring the concentration of the CO-reduced complex,[26] the spectral binding constants (K_s), and the spin states of both M11 and M11 A82W. Experimental details of the former two will be discussed below.

Determination of Spectral Binding Constants by UV−Vis Difference Spectroscopy. Spectral binding constants (K_s) for both M11 and M11 A82W with testosterone were determined by UV−vis difference spectroscopy in a fashion similar to that described previously.[19,28] Briefly, different enzyme concentrations were used (ranging from 0.5 to 10.0 μM). The enzyme was placed in the sample and reference cuvettes. The sample cuvette was titrated with 1 μL aliquots of 10 mM testosterone dissolved in DMSO. Subsequently, the reference cuvette was titrated with an equal amount of DMSO, and this was used for background correction. The DMSO concentration was always kept below 2%. After the samples had been mixed, the contents of the sample cuvette were allowed to equilibrate for 2 min prior to analysis. UV−vis difference spectra were recorded between 350 and 600 nm. The difference in absorption between 390 nm (peak) and 419 nm (trough) was plotted versus the testosterone concentration.

The spectral binding constants were determined by fitting the difference in absorption according to the formula

$$\Delta A_{390-419} = \frac{\Delta A_{\infty}[S]^n}{K_s{}^n + [S]^n} \quad (1)$$

where $\Delta A_{390-419}$ and ΔA_{∞} represent the difference in absorption between the peak and trough at a specific testosterone concentration [S] and a saturating testosterone concentration, respectively, K_s is the spectral binding constant of the enzyme−substrate complex, and n is the Hill coefficient. K_s and ΔA_{∞} were estimated by nonlinear curve fitting, using OriginPro8.

Determination of Spin States from UV Spectra. The heme iron spin state of both M11 and M11 A82W in the substrate-bound form was determined by deconvoluting absolute UV−vis spectra. Absolute UV−vis spectra were deconvoluted between 350 and 600 nm with an enzyme concentration of 500 nM and a testosterone concentration of 200 μM (concentrations were identical to those used for NMR experiments). UV−vis spectra were deconvoluted by using the multiple-Gaussian curve fitting program available in OriginPro8. Both enzymes were deconvoluted by using four components: a low-spin Soret band (419 nm), a high-spin Soret band (390 nm), δ-bands (~360 nm), and an additional "broad shoulder" between 440 and 490 nm, caused by the flavin prosthetic groups.[29]

Preparation of NMR Samples. The samples used for NMR experiments contained 50, 100, 150, or 200 μM testosterone, added from a DMSO stock solution, and 500 nM purified enzyme in 100 mM phosphate buffer (pH 7.4)

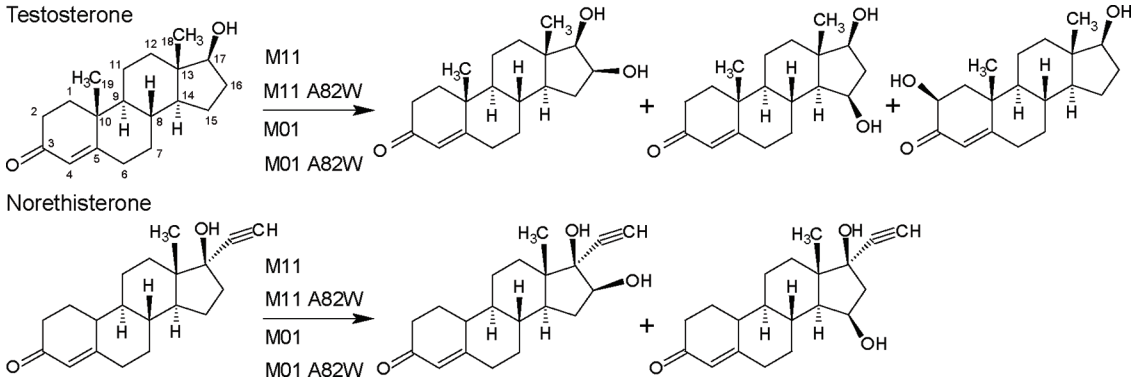

Figure 1. Chemical structures of testosterone, norethisterone, and the monohydroxy metabolites formed by P450 BM3 mutants M11, M11 A82W, M01 and M01 A82W.

with 10% D_2O for locking. As a diamagnetic control, 200 μM testosterone was dissolved in 100 mM phosphate buffer (pH 7.4). Prior to analysis, all samples were flushed with nitrogen to remove possible dissolved oxygen, which might influence the relaxation rates. The final volume of the NMR tube was 550 μL.

T_1 Relaxation Experiments. The relaxation rate ($R_1 = 1/T_1$) experiments were conducted on a Varian Unity INOVA600 and a Bruker Avance 600 spectrometer operating at a ^{1}H frequency of 599.76 MHz using a saturation recovery pulse sequence with water flip back and Watergate to suppress the water signal.[30] Eight spectra were recorded for each sample, with an interpulse delay τ ranging from 0.1 to 10 s. For each spectrum, 64 scans were acquired. The data were processed by using ACDLabs/SpecManager, version 12.01, i.e., zero filling, line broadening, phasing, baseline correction, and peak picking. OriginPro8 was used to determine R_1 relaxation rates from the peak intensities.

Deriving Distances from R_1 Relaxation Data. Under fast-exchange conditions, the longitudinal relaxation rate is the weighted average of the relaxation rates of the free and bound substrate ($R_{1,f}$ and $R_{1,b}$, respectively):[19]

$$R_{1,\mathrm{obs}} = p_f R_{1,f} + p_b R_{1,b} \tag{2}$$

where p_f and p_b are the fractions of the substrate in the free and bound state, respectively. Under the conditions of this experiment, the substrate concentration (50−200 μM) is much higher than the protein concentration (0.5 μM), so $p_f \approx 1$. $R_{1,b}$ has a contribution of both paramagnetic and diamagnetic relaxation rates ($R_{1,b} = R_{1,D} + R_{1,P}$). As discussed by Luz and Meiboom,[31] $R_{1,P}$ depends on the relaxation rate caused by the paramagnetic ion ($R_{1,M}$) and the residence time of a ligand in the active site (τ_M):

$$R_{1,\mathrm{obs}} - R_{1,f} = p_b R_{1,D} + p_b/(T_{1,M} + t_M) \tag{3}$$

Under fast-exchange conditions, $T_{1,M} \gg \tau_M$, so that $R_{1,M} = 1/T_{1,M}$ is

$$R_{1,M} = (R_{1,\mathrm{obs}} - R_{1,f} - p_b R_{1,D})/p_b \tag{4}$$

$R_{1,M}$ is related to the proton−iron distance (r_{IS}) by using the Solomon−Bloembergen equation:[32]

$$R_{1,M} = \frac{2}{15}\frac{\left(\frac{\mu_0}{4\pi}\right)^2 \gamma_I^2 \gamma_S^2 \hbar^2 S(S+1)}{r_{IS}^6}\left(\frac{3\tau_c}{1+\omega_I^2\tau_c^2} + \frac{7\tau_c}{1+\omega_S^2\tau_c^2}\right) \tag{5}$$

where μ_0 is the permeability of free space, γ_I and γ_S are the gyromagnetic ratios of the proton and electron, respectively, S is the spin state of the heme iron (obtained from deconvoluting UV−vis spectra), ω_I and ω_S are the nuclear and electronic Larmor frequencies, respectively, r_{IS} is the distance from proton nuclei to the heme iron, and τ_c is the correlation time that describes the dipolar interaction between the ligand and paramagnetic iron in solution. The correlation time τ_c mainly originates from the electron-spin relaxation time τ_S and has been estimated previously for P450 enzymes.[19,21,24] The average value of τ_c reported for P450 enzymes is 3.0e^{-10} s, and this value was used here. Note that even if the used τ_c value would be different by a factor of 2, this error would result in a systematic over- or underestimation of the calculated distances by only 10%.[21] The validity of fast exchange was confirmed from the observation of a positive temperature dependence of $R_{1,obs}$ at five temperatures (288, 293, 298, 303, and 308 K).[20,21]

Often, $R_{1,M}$ is calculated via eq 4 from $R_{1,obs}$, by subtracting the relaxation rate caused by the CO-reduced diamagnetic form of the enzyme ($R_{1,f} + p_b R_{1,D}$).[19,28] However, as noted by Smith et al.[24] and Jacobs et al.,[33] the diamagnetic relaxation rates were similar in the CO-reduced complex and enzyme-free buffer, so the diamagnetic relaxation effect caused by the enzyme ($p_b R_{1,D}$) is extremely small and can be neglected (see the Supporting Information). Therefore, eq 6 was used to calculate $R_{1,M}$

$$R_{1,M} = (R_{1,\mathrm{obs}} - R_{1,f})/p_b \tag{6}$$

where $p_b = [\mathrm{P450\ BM3}]/(K_d + [\mathrm{testosterone}])$, with K_d being the dissociation constant of the P450 BM3−testosterone complex.

In a case of multiple orientations, $R_{1,M}$ in eq 5 can be rewritten as

$$R_{1,M} \propto (f_a/r_a^6 + f_b/r_b^6 + f_c/r_c^6 + \ldots)$$

where f_a, f_b, f_c, etc., are the fractions and r_a^6, r_b^6, r_c^6, etc., the distances of orientations a, b, c, etc., respectively, in the active site. $R_{1,M}$ is therefore dominated by the term with the shortest distances. If there is one orientation present, i.e., $f_a = 1$, the

dx.doi.org/10.1021/bi201433h | Biochemistry 2012, 51, 750−760

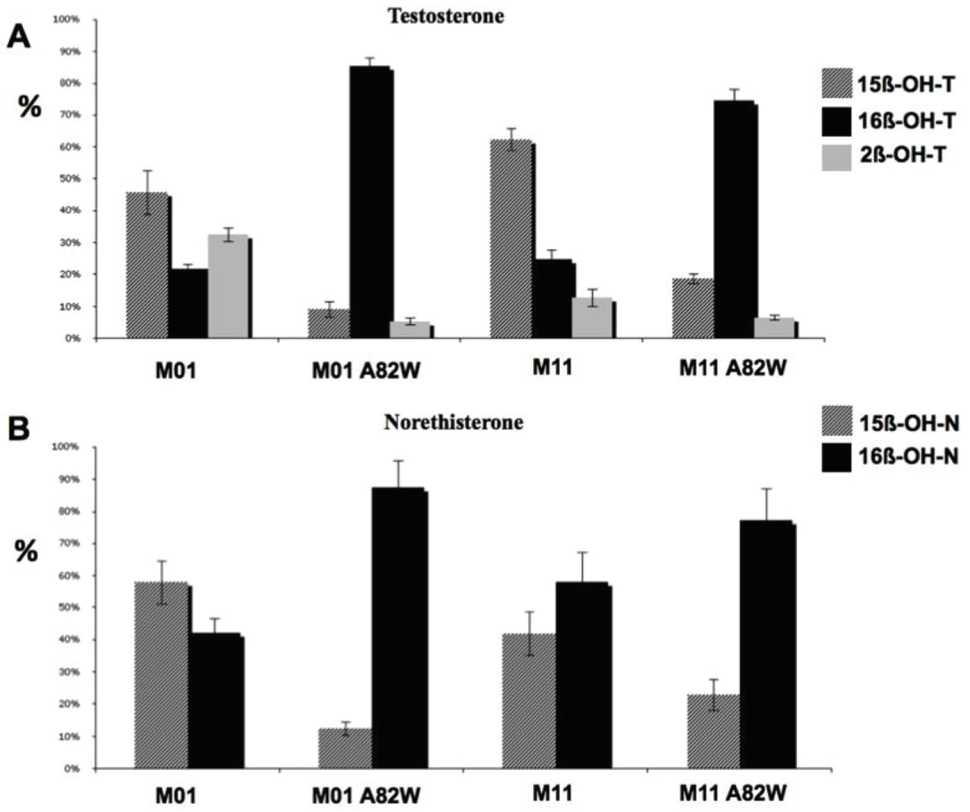

Figure 2. Relative amounts of monohydroxy metabolites of testosterone and norethisterone metabolism formed by P450 BM3 mutants M11, M11 A82W, M01, and M01 A82W. Metabolites were analyzed by UPLC with UV detection at 254 nm, and results of triplicate experiments are shown. Quantification is based on LC−UV chromatograms assuming that the extinction coefficients of the substrate and the metabolites are similar.

distances determined for all protons are representative for that specific orientation. The calculated distance corresponds to the orientation with the proton closest to the heme iron. This also implies that the distances should be internally consistent with a single orientation. Therefore, when distances are internally inconsistent, this indicates the presence of multiple orientations and suggests dynamic binding.

The r_{IS} values for each proton were calculated using eqs 2−6 with $R_{1,obs}$ and $R_{1,f}$ as input variables (for the other required parameters, see above). To obtain robust and reliable error estimates, we used Monte Carlo simulations[34,35] given the complexity of eqs 2−6. For each proton, the distance was calculated in 10000 iterations with $R_{1,obs}$, $R_{1,f}$, and spectral binding constant K_s values varying in a Gaussian distribution around their means with a width determined by the experimental errors that were determined from at least three experiments. From the resulting histograms, the average distances and distance error (standard deviation) were determined.

RESULTS

Identification of Testosterone and Norethisterone Metabolites. The structures of the testosterone and norethisterone metabolites formed by the four enzymes are displayed in Figure 1. The structures were determined on the basis of a combination of 1D ^{1}H, ^{1}H−^{1}H DQF-COSY, ^{1}H−^{13}C HSQC, ^{1}H−^{13}C HMQC, ^{1}H−^{13}C HMBC, and ^{1}H−^{1}H NOESY NMR and MS experiments. The assignments of the NMR spectra and ^{1}H and ^{13}C chemical shifts of 15β-hydroxytestosterone, 16β-hydroxytestosterone, and 2β-hydroxytestosterone are consistent with previously published data.[36,37] Details of the ^{1}H and ^{13}C NMR spectra are tabulated in the Supporting Information. Interestingly, the NOESY spectrum of 2β-hydroxytestosterone showed that the A-ring is folded into an inverted half-chair conformation, as identified by a strong NOE interaction between the proton at position 2α and the proton at position 9, which is consistent with the observations of Jacobsen et al.[38] The norethisterone metabolites were assigned to 15β-hydroxynorethisterone and 16β-hydroxynorethisterone, as recently discussed by de Vlieger et al.[15]

Effect of Mutation A82W on the Regioselectivity of Steroid Hydroxylation. To evaluate the ability of this set of mutants to oxidize steroids, incubations were first measured at a fixed substrate concentration (200 μM). Figure 2 shows the relative amounts of monohydroxy metabolites after incubation of 200 μM testosterone and norethisterone in the presence of the four studied mutants of P450 BM3. In the case of testosterone, three metabolites were produced, corresponding to 15β-hydroxytestosterone, 16β-hydroxytestosterone, and 2β-hydroxytestosterone. For both M01 and M11, the major metabolite was 15β-hydroxytestosterone. Addition of mutation A82W to both M01 and M11 resulted in a strong increase in the level of 16β-hydroxylation of testosterone. In the case of M01, mutation A82W resulted in an increase in the level of 16β-hydroxylation from 22 to 85% of total metabolism. In the case of M11, mutation A82W increased the selectivity for 16β-hydroxylation from 25 to 75%. In the case of norethisterone, two metabolites were produced, corresponding to 15β-hydroxynorethisterone and 16β-hydroxynorethisterone. As was found with testosterone, mutation A82W strongly increased selectivity for 16β-hydroxylation. In M01, mutation

dx.doi.org/10.1021/bi201433h | *Biochemistry* 2012, 51, 750−760

Table 1. Enzyme Kinetic Parameters of Metabolism of Testosterone and Norethisterone by P450 BM3 Mutants M01, M01 A82W, M11, and M11 A82W

		testosterone			norethisterone		
		K_M [a]	V_{max} [b]	V_{max}/K_M	K_M [a]	V_{max} [b]	V_{max}/K_M
M01	15β-OH	52.6 ± 5.5	0.4 ± 0.02	7.8 ± 1.2	63.4 ± 5.6	0.7 ± 0.02	10.7 ± 1.3
	16β-OH	59.5 ± 3.2	0.2 ± 0.005	3.7 ± 0.3	102.8 ± 11.2	0.8 ± 0.04	7.8 ± 0.9
	2β-OH	52.3 ± 2.5	0.3 ± 0.004	5.5 ± 0.3			
M01 A82W	15β-OH	178.2 ± 30.7	0.7 ± 0.05	3.7 ± 0.9	64.5 ± 9.8	1.2 ± 0.02	18.6 ± 3.1
	16β-OH	248.1 ± 3.9	8.5 ± 0.12	34.5 ± 1	97.4 ± 4.6	12.7 ± 0.6	130.4 ± 12.3
	2β-OH	256.7 ± 52.1	0.6 ± 0.05	2.2 ± 0.5			
M11	15β-OH	149.6 ± 20.4	18.2 ± 1.2	121.7 ± 24.6	37.5 ± 4.2	1.1 ± 0.05	29.3 ± 4.6
	16β-OH	145.1 ± 11.8	7.0 ± 0.27	48.5 ± 5.8	39.5 ± 4.6	1.6 ± 0.07	40.5 ± 6.5
	2β-OH	224.6 ± 34.5	5.8 ± 0.4	24.9 ± 5.5			
M11 A82W	15β-OH	106.7 ± 5.5	2.5 ± 0.06	23.4 ± 1.8	85 ± 12.1	1.2 ± 0.08	14.1 ± 3
	16β-OH	109.9 ± 13.6	10.2 ± 0.6	92.8 ± 16.9	100.8 ± 6.7	4.8 ± 0.3	47.6 ± 6.1
	2β-OH	99.6 ± 7.5	0.8 ± 0.03	8.1 ± 0.9			

[a] K_M values are in micromolar. [b] V_{max} values are in nanomoles of product per minute per nanomole of enzyme.

Table 2. NADPH Consumption Rates, Product Formation Rates, and Coupling Efficiencies of BM3 Mutants with Testosterone (TST) and Norethisterone (NET)

	NADPH consumption rate[a]		total product formation rate[b]		coupling efficiency (%)	
	TST	NET	TST	NET	TST	NET
M11	22.5 ± 2.2	5.4 ± 0.1	17.1 ± 0.4	2.2 ± 0.04	76 ± 9.2	41 ± 1.6
M11 A82W	10.6 ± 2.7	6.2 ± 1.3	9.2 ± 0.2	4.1 ± 0.1	83.5 ± 8.2	66.9 ± 7.2
M01	5.4 ± 0.6	4.3 ± 0.2	0.7 ± 0.03	0.6 ± 0.03	13.5 ± 2	14.2 ± 1.3
M01 A82W	11.2 ± 0.06	14.8 ± 0.7	4.3 ± 0.2	9.6 ± 0.04	38.5 ± 1.8	64.7 ± 3.5

[a] In nanomoles of NADPH per minute per nanomole of BM3. [b] In nanomoles per minute per nanomole of BM3.

A82W increased selectivity for 16β-hydroxylation from 42 to 88%; in M11, selectivity for 16β-hydroxylation increased from 58 to 77%.

Enzyme Kinetic Characterization of the P450 BM3 Mutants. To evaluate whether the strong increase in selectivity for 16β-hydroxylation was related to an increase in affinity or catalytic efficiency, we determined enzyme kinetic parameters K_M and V_{max} for all mutants with testosterone and norethisterone (Table 1).

For testosterone, mutation A82W in M01 led to a 4.2 ± 0.8-fold increase in the K_M values. The V_{max} for 16β-hydroxylation increased 42.5 times, and the catalytic efficiency (V_{max}/K_M) for 16β-hydroxylation increased 9.3 times. In the case of M11, mutation A82W led to a 1.7 ± 0.5-fold decrease in the K_M value. The V_{max} for 16β-hydroxylation increased 1.5 times, whereas for 15β-hydroxylation and 2β-hydroxylation, it decreased 7.3 times. The Hill coefficient is never significantly different from 1; therefore, cooperativity appears not to take place. In contrast to the case for testosterone, no A-ring hydroxylation was found in the case of norethisterone.

In the case of norethisterone, in M01, mutation A82W did not affect K_M values significantly. Therefore, the different selectivity was due to a change in V_{max} values. The V_{max} for 16β-hydroxylation increased 15.9-fold. In the case of M11, mutation A82W led to a 2.4 ± 0.2-fold increase in the K_M value. The V_{max} for 16β-hydroxylation increased 3-fold, while the V_{max} for 15β-hydroxylation did not change significantly. The K_M values for norethisterone are always smaller than for testosterone. Therefore, it seems that norethisterone has a higher affinity for the enzymes, although the level of product formation is higher for testosterone.

Determination of Coupling Efficiency. To evaluate the effect of the restriction of active site size on the coupling efficiency of the enzymes, the rates of NADPH consumption and product formation were measured in the presence of 200 μM testosterone and norethisterone (Table 2). For testosterone, mutation A82W in M01 led to a 2.1-fold increase in the level of NADPH consumption and to a 6.1-fold increase in the level of product formation. Thus, this mutation resulted in a 2.8-fold increase in the coupling efficiency of this enzyme. In the case of M11, after mutation A82W had been introduced, levels of both NADPH consumption and product formation decreased 2-fold; therefore, the coupling efficiency did not change significantly. For norethisterone, mutation A82W in M01 led to a 3.4-fold increase in the level of NADPH consumption and a 16-fold increase in the level of product formation, resulting in a 4.6-fold increase in coupling efficiency. In the case of M11, mutation A82W did not affect NADPH consumption significantly and led to a 1.9-fold increase in the level of product formation, which corresponds to a 1.9-fold increased coupling efficiency.

Binding Affinity and Spin State from Optical Absorption. As mentioned above, the A82W mutants of both M11 and M01 produced significantly larger amounts of 16β-hydroxytestosterone as well as of 16β-hydroxynorethisterone. For a more in-depth analysis of the metabolism in terms of binding affinity, spin state determination, and orientation of ligand in the heme active site, optical binding studies and T_1 paramagnetic relaxation NMR studies were performed. Testosterone was chosen over norethisterone because it also showed changes in 15β-hydroxylation to 16β-hydroxylation ratio as well as in D-ring to A-ring hydroxylation ratio. Its higher solubility also allows for more sensitivity in the optical and NMR experiments. In addition, the NMR spectrum of testosterone displays a smaller degree of proton resonance overlap than that of norethisterone, so that T_1 relaxation times

dx.doi.org/10.1021/bi201433h | Biochemistry 2012, 51, 750−760

can be measured more accurately. Although the increase in D-ring selectivity caused by the A82W mutation was greater for M01 than for M11, the NMR studies were performed with M11 and M11 A82W because of their higher coupling efficiency, which suggests a more productive mode of binding.

Binding of testosterone to both M11 and M11 A82W resulted in a type I binding spectrum (Figure 3) corresponding

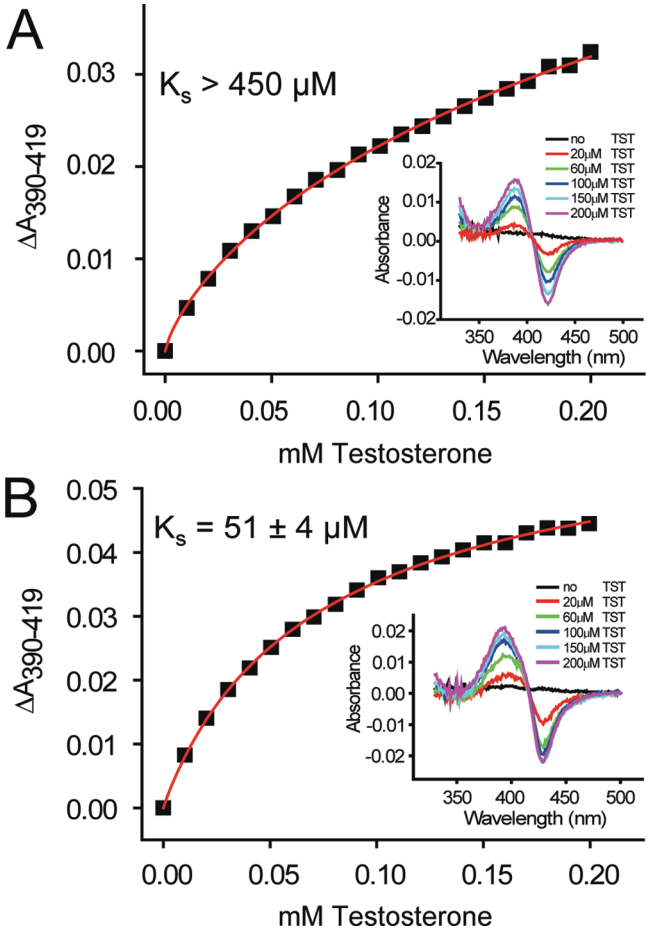

Figure 3. UV−vis difference spectra of testosterone binding to M11 (A) and M11 A82W (B).

to a substrate-induced low-spin to high-spin conversion. The spectral binding constants of testosterone binding to M11 and M11 A82W and the percentage of high-spin state in the bound form are summarized in Table 3. For M11 A82W, a dissociation

Table 3. Characteristics of Binding of Testosterone to P450 BM3 Mutants M11 and M11 A82W

	K_s (μM)[a]	Hill coefficient	high spin (%)[b]
M11	>450	0.8 ± 0.3	27
M11 A82W	51 ± 4	1.01 ± 0.04	16

[a]Spectral binding constant obtained by optical titration experiments (see Materials and Methods). [b]In the presence of 500 nM enzyme and 200 μM testosterone.

constant of 51 ± 4 μM (Table 3) was determined for testosterone with good accuracy thanks to the saturation of substrate binding being almost reached. In contrast, when testosterone was titrated to M11, no complete enzyme saturation was reached, which is indicative of a much higher dissociation constant compared to that of M11 A82W. Nevertheless, via a fit of the nonlinear curve, the spectral dissociation constant of testosterone binding to M11 was estimated to be >450 μM. This value lies outside the range of testosterone concentrations used in the titration. The highest concentration employed was 200 μM and was limited by the solubility of testosterone under our conditions. Smith et al.[24] were able to record binding spectra for a CYP2D6 mutant with testosterone concentrations of ≤1.5 mM by including 13% DMSO in the medium. However, DMSO concentrations of >2% induced strong spectral changes with our P450 BM3 mutants (data not shown), consistent with previous observations.[39] The percentages of low- and high-spin heme iron were determined by deconvolution of the absolute spectra at a protein concentration of 500 nM in the presence of 200 μM testosterone. For M11 A82W, the percentage of the high-spin form was estimated to be 16% (Table 2 and Figure S2 of the Supporting Information), while for M11, the high-spin content of substrate-bound M11 was estimated to be 27%. In the absence of testosterone, the high-spin content was estimated to be ∼10% in both enzymes.

Determination of Fast Exchange. Equation 4 assumes that $T_{1,M} \gg \tau_M$, which means that testosterone should be in fast exchange with M11 and M11 A82W. The fact that the fast-exchange conditions hold follows from the following observations. $R_{1,obs}$ of the testosterone protons increases linearly with an increasing reciprocal temperature in both M11 and M11A82W (see Figure S1 of the Supporting Information).[20,21] Titration of testosterone into a constant concentration of M11 and M11 A82W shows chemical shift changes of the methyl resonances (data not shown), which indicates fast exchange.[40] We further note that the ratio of unbound to bound substrate is around 400:1 in our case. Under these conditions, binding affects T_1 only if τ_M is not significantly smaller than $T_{1,M}$. As mentioned by Myers et al.,[41] a τ_M value of $\geq 10^{-4}$ s seems unlikely for a substrate under these circumstances.

***T*$_1$ Relaxation and Proton−Iron Distances.** The spin−lattice (R_1) relaxation rates of testosterone protons were measured in the presence and absence of M11 and M11 A82W to obtain information about the individual proton−iron distances in each mutant. Only for the protons for which the chemical shift does not overlap with those of other protons can relaxation rates be measured. Figure 4 shows the assignment of the signals in the 1D ^{1}H NMR spectrum of testosterone that do not overlap with other signals. For 11 protons, spread over the rigid testosterone structure, the relaxation rate and thus proton−iron distances could be determined. Unfortunately, the signals of protons H2*β* and H16*β*, the sites of 2*β*- and 16*β*-hydroxylation, respectively, overlapped with those of protons H6*β* and H11*β*, respectively, according to the ^{1}H−^{13}C HSQC spectrum of testosterone (Figure S5 of the Supporting Information).

Table 4 includes the relaxation rates for each proton of testosterone in the absence and presence of mutants M11 and M11 A82W and the calculated proton−iron distances. The values presented are averages and standard deviations of at least three independent experiments with 200 μM testosterone and 500 nM P450 BM3 mutant. Proton−iron distances and their corresponding standard deviations were determined by Monte Carlo simulations, in which the experimental errors originating from the relaxation rates and binding constants were simulated in a Gaussian distribution around their means.

dx.doi.org/10.1021/bi201433h | *Biochemistry* 2012, 51, 750−760

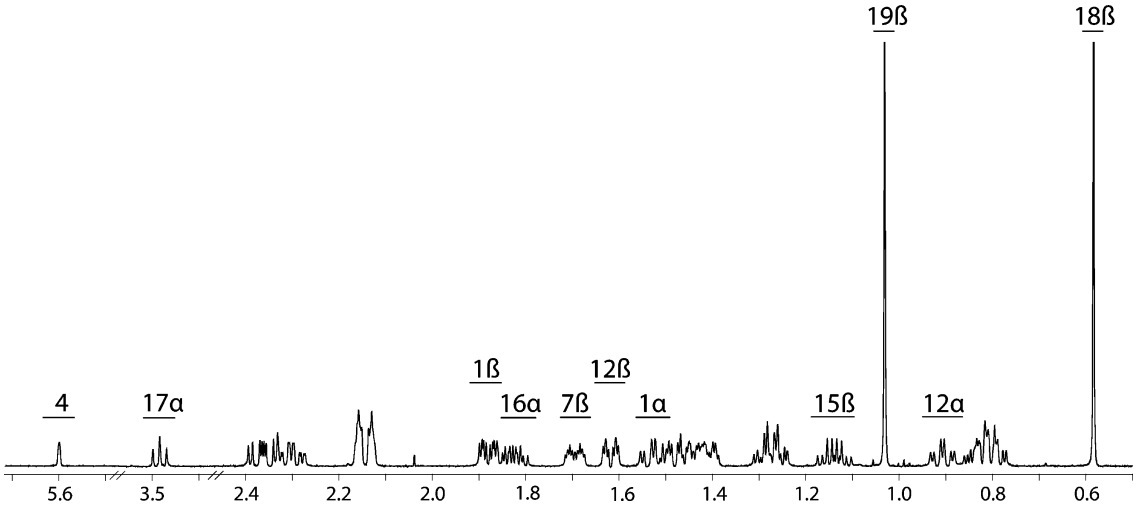

Figure 4. 1D ^{1}H NMR spectrum of testosterone in aqueous buffer. The resonances used for the T_1 NMR relaxation experiments are indicated.

Table 4. R_1 Relaxation Rates of Protons of Testosterone[a] in the Presence and Absence of M11 and M11 A82W and Calculated Proton−Iron Distances

			M11	M11 A82W	M11	M11 A82W
	ring	$R_{1,f}$ (s^{-1})[b]	$R_{1,obs}$ (s^{-1})[b]	$R_{1,obs}$ (s^{-1})[b]	r (Å)[c]	r (Å)[c]
H1α	A	1.88 ± 0.04	2.20 ± 0.07	2.19 ± 0.06	6.0 ± 0.2	6.7 ± 0.2[d]
H1β	A	2.11 ± 0.05	2.21 ± 0.08	2.19 ± 0.05	7.1 ± 0.5	8.2 ± 0.5[d]
H4	A	0.53 ± 0.01	1.26 ± 0.03	1.54 ± 0.02	5.26 ± 0.04	5.53 ± 0.02[d]
H19	A/B	1.27 ± 0.01	1.49 ± 0.01	1.76 ± 0.01	6.4 ± 0.1	6.3 ± 0.1
H7β	B	1.93 ± 0.05	2.04 ± 0.09	2.26 ± 0.07	6.9 ± 0.5	6.6 ± 0.2
H12α	C	1.90 ± 0.04	2.07 ± 0.09	2.24 ± 0.08	6.5 ± 0.2	6.5 ± 0.2
H12β	C	1.74 ± 0.03	1.86 ± 0.08	2.22 ± 0.04	6.9 ± 0.4	6.2 ± 0.1[d]
H18	C/D	1.14 ± 0.01	1.37 ± 0.02	1.72 ± 0.01	6.4 ± 0.1	6.1 ± 0.1[d]
H15β	D	1.73 ± 0.04	1.84 ± 0.09	2.11 ± 0.16	7.1 ± 0.5	6.4 ± 0.3[d]
H16α	D	1.44 ± 0.05	1.89 ± 0.12	2.23 ± 0.09	5.6 ± 0.3	5.7 ± 0.1
H17α	D	1.11 ± 0.02	1.38 ± 0.05	1.72 ± 0.03	6.2 ± 0.2	6.0 ± 0.1

[a] R_1 relaxation rates at 200 μM testosterone are shown. [b] Averages and standard deviations of R_1 relaxation rates were determined from three to five independent R_1 measurements. [c] Distances and standard deviations were estimated on the basis of Monte Carlo simulations considering the standard deviations of $R_{1,obs}$, $R_{1,f}$, and K_d. [d] Statistically significant difference in proton−iron distances between M11 and M11 A82W.

As one can see in Table 4, the shortest proton−iron distances in M11 are for the protons in the A-ring and for protons in the D-ring, while longer distances are found for the B- and C-rings. Because it is not possible to derive one specific orientation for testosterone that is consistent with all measured distances, the binding must be dynamic; i.e., testosterone must bind in multiple orientations in M11. In the case of multiple orientations, there is a possibility that each binding orientation has a different binding constant.[42] The spectral binding constant that was obtained by difference UV−vis does not provide information about the affinity of different orientations. By measuring $R_{1,obs}$ as a function of ligand concentration for each individual proton and by fitting the obtained data with eq 6, we determined previously independent estimates of the binding constant by NMR.[42] However, because of the limited solubility of testosterone and the low signal-to-noise ratios at low testosterone concentrations, we could measure the concentration dependence of $R_{1,obs}$ only over a small concentration range (100−200 μM). Although this small range and small number of data points did not permit the assessment of accurate K_d values for each proton, for each mutant no significant differences in the slope of the plot of $R_{1,obs}$ versus testosterone concentration were found for each proton (Figure S7 of the Supporting Information). This might point to comparable binding constants for each orientation. From the significantly different slopes of the $R_{1,obs}$ versus testosterone concentration curves between M11 and M11 A82W (see Figure S7), we can conclude that the affinity of testosterone for M11 is much lower than that for M11 A82W, consistent with the difference in the spectral binding constants.

Upon comparison of the proton−iron distances of testosterone bound to M11 A82W with those of M11, it is observed that the A-ring protons H1α, H1β, and H4 show small but significantly increased proton−iron distances in the M11 A82W mutant. In contrast, the distances from D-ring protons H18 and H15β to the heme iron were decreased by the A82W mutation. The results of the relaxation experiments at the lower testosterone concentrations were consistent to those obtained at 200 μM testosterone. Again, the introduction of the A82W mutation was shown to cause an increase in the proton−iron distances of A-ring protons and a decrease in the proton−iron distances of some D-ring protons (data not shown). Because of the better signal-to-noise ratios, Table 4 shows only the results obtained at 200 μM testosterone.

dx.doi.org/10.1021/bi201433h | *Biochemistry* 2012, 51, 750−760

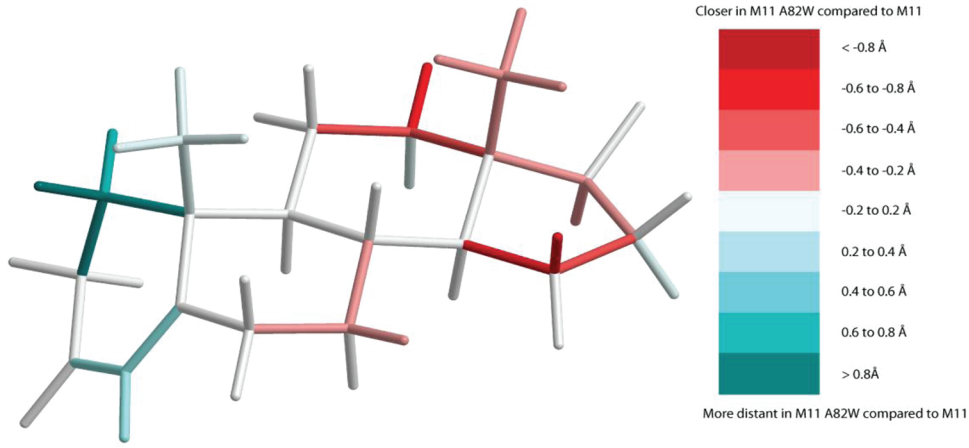

Figure 5. Differences in distances for binding of testosterone to M11 and M11 A82W. The protons for which proton−iron distances were derived are colored according to the difference in distance (see the legend). The directly attached carbon and C−H bond are colored like the proton. Protons for which no proton−iron distance could be derived are colored white. A negative difference in distance (reddish) means a shorter proton−iron distance in M11 A82W than in M11. A positive difference in distance (blueish) means a longer proton−iron distance in M11 A82W than in M11.

DISCUSSION

Because hydroxysteroids have important pharmaceutical applications, there is a great need for biocatalysts with high activity and regioselectivity in steroid hydroxylation. Recently, by laboratory evolution starting from P450 BM3 (F87A) mutants were obtained with high selectivity for 2β- and 15β-hydroxylation.[23] In the work presented here, we present two novel P450 BM3 enzymes, M01 A82W and M11 A82W, which can catalyze regioselective hydroxylation of steroids at position 16β. The importance for modification of steroids at this position has been discussed previously by Laplante et al.[45] and Vicker et al.[46]

Huang et al.[16] previously showed that substitution of alanine 82 in wild-type P450 BM3 with the larger and more hydrophobic amino acids, tryptophan and phenylalanine, improves binding affinity and K_M for long-chain fatty acids by orders of magnitude. In this study, we demonstrate that substitution of alanine 82 with tryptophan in P450 BM3 mutants M01 and M11 results in improved regioselectivity and catalytic efficiency of testosterone hydroxylation. The binding affinity of testosterone for M11 A82W is significantly higher than its binding affinity for M11 (Table 3), which might be explained by the addition of a hydrophobic interaction between testosterone and the tryptophan at position 82. A more efficient exclusion of water from the active site by the stronger substrate−enzyme interaction might also explain the increased coupling efficiency of the A82W mutants (Table 2). Uncoupling of the catalytic cycle of P450s can occur when mutations are introduced into the active site of P450 or in the presence of non-native substrates,[43] leading to the formation of reactive oxygen species and rapid enzyme inactivation.[8] Interestingly, the recently published P450 BM3 mutants with high selectivity for 2β- and 15β-hydroxylation of testosterone also contained substitutions at position 82, including the A82F substitution.[47] However, only small amounts of 16β-hydroxy-testosterone were found. In this study, mutations at position 82 were always combined with mutations at position 78, because this combination was expected to act synergistically. Therefore, the simultaneous mutation at position 78 might explain the preference for 15β-hydroxylation.

T_1 NMR relaxation experiments were performed to investigate whether mutation A82W leads to changes in proton−iron distances that might reflect differences in the orientation and dynamics of testosterone in the active sites of M11 and M11 A82W. Using the same approach, Smith et al.[22] previously studied the orientation of binding of testosterone to a CYP2D6 mutant that had acquired the ability to catalyze testosterone hydroxylation by an F483I mutation. In this study, first the proton resonances of testosterone were assigned on the basis of DQF-COSY, ^{1}H−^{13}C HSQC, ^{1}H−^{1}H NOESY, and 1D ^{1}H NMR spectra. All assignments were consistent with those of Kirk et al.[37] On the basis of our assignments, we conclude that a number of resonances were incorrectly assigned by Smith et al.,[22] as detailed in the Supporting Information. In particular, the signals of the protons at positions 2β and 16β, which are two of the sites of hydroxylation by BM3 mutants, appeared to overlap with the resonances of other protons, excluding the possibility of determining relaxation rates for these protons.

As shown in Table 4, for M11 the shortest proton−iron distances are obtained for protons located in the A- and D-rings (H1α, H4, and H16α). The fact that it is not possible to assign a specific orientation of testosterone in M11 that is consistent with all measured distances implies that the binding must be dynamic; i.e., testosterone is able to bind in multiple orientations. The distance data, which are well spread over the rigid testosterone, appear to be consistent with two classes of orientations of testosterone in the M11 active site, namely, a group of orientations with the A-ring closest to the heme iron and a group of orientations with the D-ring closest to the heme iron. Also, in the case of M11 A82W, the distances imply the presence of multiple orientations and dynamics involved in binding. Statistically significant differences in testosterone orientation were found upon comparison of M11 A82W with M11, as visualized in Figure 5. In M11 A82W, protons H1α, H1β, and H4 moved farther from the heme iron, whereas H12β, H15β, and H18β moved closer to the heme iron. Although the change in substrate orientation is mainly deduced by changes in distances of protons that are not hydroxylated, the changes are consistent with the increased selectivity for D-ring hydroxylation and reduced selectivity for A-ring hydroxylation for M11 A82W. The decrease in 15β-hydroxylation in

dx.doi.org/10.1021/bi201433h | *Biochemistry* 2012, 51, 750−760

the M11 A82W mutant relative to that in M11 (Figure 2) might be explained by an orientation of the D-ring in which H16β is able to approach the heme iron significantly closer than H15β. Alternatively, the C−H16β bond might orient in a more favorable position for abstraction of hydrogen by the reactive FeO species: a linear C−H−O arrangement is considered a typical feature in C−H bond activation by FeO species, which precedes aliphatic hydroxylation.[45] In both cases, H16β will be the preferred site of hydroxylation at the expense of H15β hydroxylation. Unfortunately, it was not possible to determine the difference in distances between the heme iron and the H15β and H16β protons, because the signal of the latter proton overlaps with that of proton H11β.

From the distance data, it can be seen that the average proton−iron distances of testosterone in M11 and M11 A82W are 6.3 Å, while the shortest distances are ∼5.3 Å. A distance of <4 Å is considered to be necessary to allow hydrogen abstraction.[44] However, it should be realized that the proton−iron distances in Table 4 represent binding of testosterone to the initial ferric enzyme−substrate complexes that do not necessarily represent the orientation of testosterone in the oxygenated ferrous form of P450 BM3. It has been shown previously that fatty acids bind P450 BM3 enzymes via a two-step binding process, with initial binding to a site distant from the heme iron and movement closer to the heme iron upon iron reduction.[44] Nonflexible compounds like codeine and testosterone were considered to bind via a one-step binding mechanism to CYP2D6 (class I P450).[22] The question of whether nonflexible ligands, like steroids, bind in P450 BM3 enzymes via a two-step binding mechanism or directly to the proximal position then arises. The average distances and shortest distances for binding of testosterone to M11 and M11 A82W indicate that testosterone binds distant in the non-reduced form in both enzymes, similar to fatty acids binding to nonreduced P450 BM3.[19] Thus, it is most likely that steroids bind to P450 BM3 enzymes via a two-step binding mechanism.

In summary, we showed that applying substitution A82W to P450 BM3 mutants M01 and M11 improves regioselective hydroxylation of norethisterone and testosterone at position 16β. This mutation improved both binding affinity and coupling efficiency, thereby strongly improving the catalytic activity. As shown by T_1 paramagnetic relaxation NMR, this single mutation appears to change the orientation of testosterone in the M11 A82W mutant as compared to the orientation in M11. Testosterone is oriented in M11 with both the A- and D-rings closest to the heme iron, whereas testosterone is mainly oriented with its D-ring closest to the heme iron in the M11 A82W mutant, which might explain its increased selectivity for D-ring hydroxylation.

■ ASSOCIATED CONTENT

Supporting Information

Details of the ^{1}H and ^{13}C NMR spectra of 2β-, 15β-, and 16β-testosterone, rationalization of the small contribution of the diamagnetic relaxation effect caused by the enzymes, demonstration of fast exchange by a positive linear dependence of $R_{1,obs}$ as a function of testosterone concentration, deconvolution of absolute absorbance spectra to determine the percentages of low- and high-spin heme iron, correction of the assignment of ^{1}H NMR spectra of testosterone as published by Smith et al.,[24] examples of Monte Carlo simulations used to determine proton−iron distances and their standard deviations, and concentration dependence of $R_{1,obs}$ of testosterone in M11 and M11 A82W. This material is available free of charge via the Internet at http://pubs.acs.org.

■ AUTHOR INFORMATION

Corresponding Author

*Telephone: +31-205987595. E-mail: j.n.m.commandeur@vu.nl.

Author Contributions

V.R. and A.J.K. contributed equally to this work.

Funding

This research was performed within the framework of Project D2-102 of the Dutch Top Institute Pharma.

■ ABBREVIATIONS

CYP, cytochrome P450; NMR, nuclear magnetic resonance; P450 BM3, cytochrome P450 BM3 (CYP102A1).

■ REFERENCES

(1) Guengerich, F. P. (2001) Common and uncommon cytochrome P450 reactions related to metabolism and chemical toxicity. *Chem. Res. Toxicol. 14*, 611−650.

(2) Guengerich, F. P. (2002) Cytochrome P450 enzymes in the generation of commercial products. *Nat. Rev. Drug Discovery 1*, 359−366.

(3) Bernhardt, R. (2006) Cytochromes P450 as versatile biocatalysts. *J. Biotechnol. 124*, 128−145.

(4) Urlacher, V., and Schmid, R. D. (2002) Biotransformations using prokaryotic P450 monooxygenases. *Curr. Opin. Biotechnol. 13*, 557−564.

(5) Sawayama, A. M., Chen, M. M., Kulanthaivel, P., Kuo, M. S., Hemmerle, H., and Arnold, F. H. (2009) A panel of cytochrome P450 BM3 variants to produce drug metabolites and diversify lead compounds. *Chemistry 15*, 11723−11729.

(6) Fernandes, P., Cruz, A., Angelova, B., Pinheiro, H. M., and Cabral, J. M. S. (2003) Microbial conversion of steroid compounds: Recent developments. *Enzyme Microb. Technol. 32*, 688−705.

(7) Agematu, H., Matsumoto, N., Fujii, Y., Kabumoto, H., Doi, S., Machida, K., Ishikawa, J., and Arisawa, A. (2006) Hydroxylation of testosterone by bacterial cytochromes P450 using the *Escherichia coli* expression system. *Biosci., Biotechnol., Biochem. 70*, 307−311.

(8) Munro, A. W., Leys, D. G., McLean, K. J., Marshall, K. R., Ost, T. W., Daff, S., Miles, C. S., Chapman, S. K., Lysek, D. A., Moser, C. C., Page, C. C., and Dutton, P. L. (2002) P450 BM3: The very model of a modern flavocytochrome. *Trends Biochem. Sci. 27*, 250−257.

(9) Peters, M. W., Meinhold, P., Glieder, A., and Arnold, F. H. (2003) Regio- and enantioselective alkane hydroxylation with engineered cytochromes P450 BM-3. *J. Am. Chem. Soc. 125*, 13442−13450.

(10) Lussenburg, B. M. A., Babel, L., Vermeulen, N. P. E., and Commandeur, J. N. M. (2005) Evaluation of alkoxyresorufins as fluorescent substrates for high-throughput screening of cytochrome P450BM3 and site-directed mutants. *Drug Metab. Rev. 37*, 20−21.

(11) Lewis, J. C., Mantovani, S. M., Fu, Y., Snow, C. D., Komor, R. S., Wong, C. H., and Arnold, F. H. (2010) Combinatorial alanine substitution enables rapid optimization of cytochrome P450(BM3) for selective hydroxylation of large substrates. *ChemBioChem 11*, 2502−2505.

(12) Lewis, J. C., Bastian, S., Bennett, C. S., Fu, Y., Mitsuda, Y., Chen, M. M., Greenberg, W. A., Wong, C. H., and Arnold, F. H. (2009) Chemoenzymatic elaboration of monosaccharides using engineered cytochrome P450BM3 demethylases. *Proc. Natl. Acad. Sci. U.S.A. 106*, 16550−16555.

(13) van Vugt-Lussenburg, B. M. A., Damsten, M. C., Maasdijk, D. M., Vermeulen, N. P. E., and Commandeur, J. N. M. (2006) Heterotropic and homotropic cooperativity by a drug-metabolising

mutant of cytochrome P450 BM3. *Biochem. Biophys. Res. Commun. 346*, 810−818.
(14) van Vugt-Lussenburg, B. M. A., Stjernschantz, E., Lastdrager, J., Oostenbrink, C., Vermeulen, N. P. E., and Commandeur, J. N. M. (2007) Identification of critical residues in novel drug metabolizing mutants of cytochrome P450 BM3 using random mutagenesis. *J. Med. Chem. 50*, 455−461.
(15) de Vlieger, J. S., Kolkman, A. J., Ampt, K. A., Commandeur, J. N. M., Vermeulen, N. P. E., Kool, J., Wijmenga, S. S., Niessen, W. M., Irth, H., and Honing, M. (2010) Determination and identification of estrogenic compounds generated with biosynthetic enzymes using hyphenated screening assays, high resolution mass spectrometry and off-line NMR. *J. Chromatogr., B: Anal. Technol. Biomed. Life Sci. 878*, 667−674.
(16) Huang, W. C., Westlake, A. C., Marechal, J. D., Joyce, M. G., Moody, P. C., and Roberts, G. C. (2007) Filling a hole in cytochrome P450 BM3 improves substrate binding and catalytic efficiency. *J. Mol. Biol. 373*, 633−651.
(17) Vottero, E., Rea, V., Lastdrager, J., Vermeulen, N. P. E., and Commandeur, J. N. M. (2011) Role of residue 87 in substrate- and regioselectivity of drug metabolizing cytochrome P450 CYP102A1M11. *J. Biol. Inorg. Chem. 16*, 899−912.
(18) Yao, H., McCullough, C. R., Costache, A. D., Pullela, P. K., and Sem, D. S. (2007) Structural evidence for a functionally relevant second camphor binding site in P450cam: Model for substrate entry into a P450 active site. *Proteins 69*, 125−138.
(19) Modi, S., Primrose, W. U., Boyle, J. M. B., Gibson, C. F., Lian, L. Y., and Roberts, G. C. K. (1995) NMR-Studies of substrate-binding to cytochrome-P-450 (BM3): Comparisons to cytochrome-P-450 (Cam). *Biochemistry 34*, 8982−8988.
(20) Regal, K. A., and Nelson, S. D. (2000) Orientation of caffeine within the active site of human cytochrome P450 1A2 based on NMR longitudinal (T-1) relaxation measurements. *Arch. Biochem. Biophys. 384*, 47−58.
(21) Cameron, M. D., Wen, B., Allen, K. E., Roberts, A. G., Schuman, J. T., Campbell, A. P., Kunze, K. L., and Nelson, S. D. (2005) Cooperative binding of midazolam with testosterone and α-naphthoflavone within the CYP3A4 active site: A NMR T-1 paramagnetic relaxation study. *Biochemistry 44*, 14143−14151.
(22) Oliver, C. F., Modi, S., Sutcliffe, M. J., Primrose, W. U., Lian, L. Y., and Roberts, G. C. K. (1997) A single mutation in cytochrome P450 BM3 changes substrate orientation in a catalytic intermediate and the regiospecificity of hydroxylation. *Biochemistry 36*, 1567−1572.
(23) Oliver, C. F., Modi, S., Primrose, W. U., Lian, L. Y., and Roberts, G. C. K. (1997) Engineering the substrate specificity of *Bacillus megaterium* cytochrome P-450 BM3: Hydroxylation of alkyl trimethylammonium compounds. *Biochem. J. 327*, 537−544.
(24) Smith, G., Modi, S., Pillai, I., Lian, L. Y., Sutcliffe, M. J., Pritchard, M. P., Friedberg, T., Roberts, G. C., and Wolf, C. R. (1998) Determinants of the substrate specificity of human cytochrome P-450 CYP2D6: Design and construction of a mutant with testosterone hydroxylase activity. *Biochem. J. 331* (Part 3), 783−792.
(25) Damsten, M. C., van Vugt-Lussenburg, B. M. A., Zeldenthuis, T., de Vlieger, J. S. B., Commandeur, J. N. M., and Vermeulen, N. P. E. (2008) Application of drug metabolising mutants of cytochrome P450BM3 (CYP102A1) as biocatalysts for the generation of reactive metabolites. *Chem.-Biol. Interact. 171*, 96−107.
(26) Omura, T., and Sato, R. (1964) Carbon Monoxide-Binding Pigment of Liver Microsomes. I. Evidence for Its Hemoprotein Nature. *J. Biol. Chem. 239*, 2370−2378.
(27) Truan, G., and Peterson, J. A. (1998) Thr268 in substrate binding and catalysis in P450BM-3. *Arch. Biochem. Biophys. 349*, 53−64.
(28) Hummel, M. A., Gannett, P. M., Aguilar, J., and Tracy, T. S. (2008) Substrate proton to heme distances in CYP2C9 allelic variants and alterations by the heterotropic activator, dapsone. *Arch. Biochem. Biophys. 475*, 175−183.
(29) Li, H. Y., Darwish, K., and Poulos, T. L. (1991) Characterization of recombinant *Bacillus megaterium* Cytochrome-P-450BM-3 and its two functional domains. *J. Biol. Chem. 266*, 11909−11914.
(30) Liu, M. L., Mao, X. A., Ye, C. H., Huang, H., Nicholson, J. K., and Lindon, J. C. (1998) Improved WATERGATE pulse sequences for solvent suppression in NMR spectroscopy. *J. Magn. Reson. 132*, 125−129.
(31) Luz, Z., and Meiboom, S. (1964) Proton relaxation in dilute solutions of cobalt(2) + nickel(2) ions in methanol: Rate of methanol exchange of solvation sphere. *J. Chem. Phys. 40*, 2686−&2692.
(32) Solomon, I., and Bloembergen, N. (1956) Nuclear magnetic interactions in the Hf molecule. *J. Chem. Phys. 25*, 261−266.
(33) Jacobs, R. E., Singh, J., and Vickery, L. E. (1987) NMR Studies of cytochrome-P-450scc: Effects of steroid binding on water proton access to the active-site of the ferric enzyme. *Biochemistry 26*, 4541−4545.
(34) Bevington, P. R. (1992) *Data reduction and error analysis for the pysical sciences*, McGraw-Hill, London.
(35) Press, W. H. (2007) Random numbers. *Numerical recipes: The art of scientific computing*, Chapter 7, Cambridge University Press, Cambridge, U.K.
(36) Mahato, S. B., and Mukherjee, A. (1984) Microbial transformation of testosterone by *Aspergillus fumigatus*. *J. Steroid Biochem. 21*, 341−342.
(37) Kirk, D. N., Toms, H. C., Douglas, C., White, K. A., Smith, K. E., Latif, S., and Hubbard, R. W. P. (1990) A survey of the high-field H-1-NMR spectra of the steroid-hormones, their hydroxylated derivatives, and related-compounds. *J. Chem. Soc., Perkin Trans. 2*,, 1567−1594.
(38) Jacobsen, N. E., Kover, K. E., Murataliev, M. B., Feyereisen, R., and Walker, F. A. (2006) Structure and stereochemistry of products of hydroxylation of human steroid hormones by a housefly cytochrome P450 (CYP6A1). *Magn. Reson. Chem. 44*, 467−474.
(39) Roccatano, D., Wong, T. S., Schwaneberg, U., and Zacharias, M. (2005) Structural and dynamic properties of cytochrome P450BM-3 in pure water and in a dimethylsulfoxide/water mixture. *Biopolymers 78*, 259−267.
(40) Jardetzky, O., and Roberts, G. C. K. (1981) *NMR in Molecular Biology*, Academic Press, New York.
(41) Myers, T. G., Thummel, K. E., Kalhorn, T. F., and Nelson, S. D. (1994) Preferred orientations in the binding of 4′-hydroxyacetanilide (acetaminophen) to cytochrome-P450 1a1 and 2b1 isoforms as determined by C-13-NMR and N-15-NMR relaxation studies. *J. Med. Chem. 37*, 860−867.
(42) Modi, S., Gilham, D. E., Sutcliffe, M. J., Lian, L. Y., Primrose, W. U., Wolf, C. R., and Roberts, G. C. K. (1997) 1-Methyl-4-phenyl-1,2,3,6-tetrahydropyridine as a substrate of cytochrome P450 2D6: Allosteric effects of NADPH-cytochrome P450 reductase. *Biochemistry 36*, 4461−4470.
(43) Loida, P. J., and Sligar, S. G. (1993) Engineering Cytochrome-P-450 (Cam) to increase the stereospecificity and coupling of aliphatic hydroxylation. *Protein Eng. 6*, 207−212.
(44) Modi, S., Sutcliffe, M. J., Primrose, W. U., Lian, L. Y., and Roberts, G. C. K. (1996) The catalytic mechanism of cytochrome P450 BM3 involves a 6 Å movement of the bound substrate on reduction. *Nat. Struct. Biol. 3*, 414−417.
(45) Kamachi, T., and Yoshizawa, K. (2003) A theoretical study on the mechanism of camphor hydroxylation by compound I of cytochrome p450. *J. Am. Chem. Soc. 125*, 4652−4661.
(46) Vicker, N., Lawrence, H. R., Allan, G. M., Bubert, C., Smith, A., Tutill, H. J., Purohit, A., Day, J. M., Mahon, M. F., Reed, M. J., and Potter, B. V. L. (2006) Focused libraries of 16-substituted estrone derivatives and modified E-ring steroids: Inhibitors of 17 beta-hydroxysteroid dehydrogenase type 1. *ChemMedChem 1*, 464−481.
(47) Kille, S., Zilly, F. E., Acevedo, J. P., and Reetz, M. T. (2011) Regio- and stereoselectivity of P450-catalysed hydroxylation of steroids controlled by laboratory evolution. *Nat. Chem. 3*, 738−743.